

## Research Article

# Quantification of Surface Amorphous Content Using Dispersive Surface Energy: the Concept of Effective Amorphous Surface Area

Jeffrey Brum<sup>1,3</sup> and Daniel Burnett<sup>2</sup>

Received 9 March 2011; accepted 20 June 2011; published online 2 July 2011

**Abstract.** We investigate the use of dispersive surface energy in quantifying surface amorphous content, and the concept of effective amorphous surface area is introduced. An equation is introduced employing the linear combination of surface area normalized square root dispersive surface energy terms. This equation is effective in generating calibration curves when crystalline and amorphous references are used. Inverse gas chromatography is used to generate dispersive surface energy values. Two systems are investigated, and in both cases surface energy data collected for physical mixture samples comprised of amorphous and crystalline references fits the predicted response with good accuracy. Surface amorphous content of processed lactose samples is quantified using the calibration curve, and interpreted within the context of effective amorphous surface area. Data for bulk amorphous content is also utilized to generate a thorough picture of how disorder is distributed throughout the particle. An approach to quantifying surface amorphous content using dispersive surface energy is presented. Quantification is achieved by equating results to an effective amorphous surface area based on reference crystalline, and amorphous materials.

**KEY WORDS:** amorphous; dispersive surface energy; IGC; quantification.

## INTRODUCTION

Inverse gas chromatography (IGC) has been applied to a number of surface characterization problems involving drug substances and excipients, as well as other materials. Specific pharmaceutical examples include: surface energy and acid–base parameter determination (1), examining glass transitions (2), and solubility parameter determination for excipient selection (3,4). Of particular interest has been employing IGC to characterize the surface energy differences between amorphous and crystalline states for a given material (5). Typically, the dispersive energy value of the amorphous surface which is higher than that of the crystalline surface consistent with the elevated free energy of the amorphous solid phase as a whole. When physical mixtures of amorphous and crystalline materials have been examined by IGC results have lead to questions about the respective role of “high” (*i.e.* amorphous) and “low” (*i.e.* crystalline) energy sites during the course of the measurement, particularly at infinite dilution (6). These questions arise to a significant extent from the fact that correlating dispersive surface energy ( $\gamma_S^D$ ) to the fraction of amorphous content for a series of physical mixtures will not result in a straight line or other simple function. Even when the physical mixtures are normalized to

the surface area present for the respective amorphous and crystalline components, a linear response has not been reported (7). This has led to some discussion as to the physical role of “high” vs “low” energy sites. Ultimately, the surface is an ensemble of energetic states with regards to potential adsorption sites. These states will affect the surface residence time for a given probe molecule as a function of the energetics of sorption for that particular probe-site interaction by  $\tau = \tau_0 e^{Q/RT}$ , where  $\tau_0$  is a constant,  $R$  is the universal gas constant,  $T$  is the temperature, and  $Q$  is the energy of interaction (8). In terms of surface interactions, it is not possible for a probe to preferentially interact with a site based on the energy involved, rather probes will sample all surface available. Higher energy interactions exert their influence by longer residence times of probes physisorbed to the surface. With all other things being equal (*e.g.* surface area) a higher population of higher energy sites will manifest itself as a longer retention time in an IGC experiment.

In terms of further understanding how to interpret dispersive surface energy data obtained from physical mixtures of crystalline and amorphous phases, it is important to revisit the fundamental relationship between the work of adhesion (for a particular probe surface interaction), and the *non-probe-specific* concept of dispersive surface energy. An investigation by Sun and Berg (9) evaluating the effective surface energy of heterogeneous mixtures produced the framework to understand  $\gamma_S^D$  values obtained from samples comprised of two materials with different values of  $\gamma_S^D$ . The procedure can be easily applied to mixtures of crystalline and amorphous phases, as long as the crystalline and amorphous phases have measurably different dispersive surface energy

<sup>1</sup> Physical Properties, Particle Generation, Engineering and Control, Product Development, GlaxoSmithKline Pharmaceuticals, 1250 S. Collegeville Road, Collegeville, Pennsylvania 19426, USA.

<sup>2</sup> Surface Measurement Systems Ltd., Allentown, Pennsylvania, USA.

<sup>3</sup> To whom correspondence should be addressed. (e-mail: jeffrey.brum@gsk.com)

values. Further, this approach can be adapted to quantify surface amorphous content for an unknown sample which may contain a mixture of crystalline and disordered states; for example, a sample which has been milled using micronization. In this report, we develop this approach above and apply it to two systems:  $\alpha$ -lactose monohydrate/amorphous lactose and crystalline drug substance A/amorphous drug substance A. Using  $\gamma_S^D$  to quantify surface amorphous content requires the additional concept of effective amorphous surface area (EASA) to make appropriate use of the results. To understand the results for processed lactose samples studied here, the idea of EASA will be discussed. Subsequently, we utilize solution calorimetry to evaluate the bulk amorphous content of lactose thereby producing an example of how the combination of bulk and surface techniques can produce a more complete picture of how disorder is distributed within a particle. This represents an important approach to separating and characterizing bulk vs. surface disorder since the level of disorder at the surface of a particle may be quite different than that distributed in the bulk.

## MATERIALS

### Lactose

$\alpha$ -Lactose monohydrate was obtained from J.T. Baker (ACS reagent grade) and was used as received. Spray-dried lactose (amorphous) was prepared using a Yamato GB 22 spray dryer with water as the solvent. The inlet temperature was 150°C, and an outlet temperature of 75°C was used. During the course of the study, the lactose spray-dried powder (SDP) was kept over desiccant at reduced pressure to inhibit crystallization.

### Drug Substance A

The crystalline reference was prepared by recrystallization from a solution in heated water to which acetone was added during cooling. The amorphous reference sample was prepared by ball milling. A Retsch Mixer Mill with stainless steel grinding jar and balls was used with a milling time of 5 h. This sample was stored over desiccant.

## METHODS

### IGC

For the IGC experiments in this study, the samples (200–300 mg) were packed into silanised glass columns (30 cm long, 4.0 mm ID). Prior to measurement the sample was pre-treated at 303 K for 5 h *in situ* at 0% RH. IGC measurements were carried out using the SMS-IGC 2000 system (Surface Measurement Systems, UK). The samples were measured at 303 K with a helium carrier gas flow rate of 10 ml/min. Probe molecules were decane, nonane, octane, heptane, and hexane. All solvents were supplied by Aldrich and were HPLC grade. The probe molecules were injected from the headspace via loops with 135- or 250- $\mu$ l volumes. The injection concentration was 0.05 p/p<sub>0</sub>. The deadtime was determined by a methane injection.

Surface energy can be divided into dispersive and specific contributions. The former is due to Lifshitz—van der Waals interactions and the latter is related to polar interactions (10). The dispersive surface energy is the focus of the current work, and can be determined directly with IGC by injection of a homologous series of alkanes. The retention time of each injected probe vapor depends on the strength of interaction with the surface: the stronger the interaction, the higher the retention time. The gross retention time,  $t_R$  obtained from the maximum (or the center of mass) of the eluted peak has to be corrected for the deadtime,  $t_0$  of the system. The deadtime is the time a non-interacting probe takes to pass through the IGC system and packed column. If the deadtime is subtracted the net retention time is obtained and can be transformed into the retention volume,  $V_N$  via Eq. 1.

$$V_N = j/m \cdot F \cdot (t_R - t_0) \cdot \frac{T}{273.15} \quad (1)$$

where  $T$  is the column temperature,  $m$  is the sample mass,  $F$  is the exit flow rate at 1 atm, and  $j$  is the James-Martin correction, which corrects the retention time for the pressure drop in the column bed. The net retention volume of each alkane injection is related to the dispersive surface energy,  $\gamma_S^D$  via Eq. 2.

$$RT \ln V_N = 2N_A (\gamma_S^D)^{1/2} a (\gamma_L^D)^{1/2} + \text{const.} \quad (2)$$

In Eq. 2  $N_A$  is the Avogadro constant,  $R$  is the gas constant,  $\gamma_L^D$  is the dispersive surface tension of the probe, and  $a$  the cross-sectional area of the probe. If the term  $RT \ln V_N$  for a range of injected alkanes is plotted versus  $a (\gamma_L^D)^{1/2}$ , a straight line results and the dispersive surface energy can be calculated from the slope of the corresponding linear fit (11).

### BET Surface Area $N_2$ Adsorption

For lactose, a Micromeritics Gemini 2375 surface area analyzer was employed using  $N_2$  gas as the probe. For drug substance A a Micromeritics Tristar system was employed also with  $N_2$  as the probe. Data was collected over a p/p<sub>0</sub> range of 0.05–0.3. The surface area was calculated based on the linear form of the BET equation.

### Solution Calorimetry

A Thermometric (Thermometric AB, Sweden) 2225 Precision Solution Calorimeter was used to collect enthalpies of solution for certain lactose samples in this study. The calorimeter was used in conjunction with a Thermometric model 2277 Thermal Activity Monitor. Of the sample, 100–200 mg was used for each analysis with water as the solvent. The bath temperature was 25.00°C, and a stir rate of 600 rpm was used.

### X-Ray Powder Diffraction

X-ray powder diffraction (XRPD) patterns were collected on a Panalytical X'Pert Pro Diffractometer using Cu K $\alpha$  radiation operated in reflection mode to capture the 2 $\theta$  range of 2° to 40° using a step size of 0.0167 2 $\theta$ .

## THEORETICAL

The following is an outline of what has previously been developed by Sun and Berg for understanding dispersive surface energy results from measurements on heterogeneous mixtures of materials with different surface energies (9). We start with the relationship of the retention volume ( $V_N$ ) and standard free energy ( $\Delta G_{\text{ads}}^0$ ) of adsorption.  $V_N$  as defined in Eq. 1 is the fundamental measurement of an IGC instrument and is the volume of carrier gas necessary to fully elute a probe gas from the sample. It is directly related to  $\Delta G_{\text{ads}}^0$  via Eq. 3.

$$RT \ln V_N = -\Delta G_{\text{ads}}^0 + C \quad (3)$$

where  $C$  is a constant related to specific experimental considerations,  $R$  is the universal gas constant, and  $T$  is the measurement temperature in Kelvin. When restricting to only van der Waals interactions, the work of adhesion between the probe and surface ( $W_a$ ) can be given as Eq. 4.

$$W_a = W_a^D = 2(\gamma_S^D \gamma_L^D)^{1/2} = \frac{-\Delta G_{\text{ads}}^0}{aN_A} \quad (4)$$

where  $\gamma_S^D$  is the dispersive surface energy of the solid,  $\gamma_L^D$  is the dispersive surface tension of the liquid probe molecule, and  $a$  is the cross-sectional area of the probe molecule. Combining Eqs. 3 and 4 produces the equation commonly used to establish  $\gamma_S^D$  when a series of homologous alkanes are employed in an IGC experiment (This is the same as Eq. 2).

$$RT \ln V_N = 2aN_A(\gamma_S^D \gamma_L^D)^{1/2} + C \quad (5)$$

When two surfaces are present (*e.g.*, a physical mixture of crystalline and amorphous solids), we expect the total work of adhesion of the probe with the solid phase to be a linear combination of terms:

$$W_a = \phi_1 W_{a1} + \phi_2 W_{a2} \quad (6)$$

Here  $\phi_x$  are the respective surface fractions of each solid. It is important to note that where we are developing this argument based on two components, the argument is in fact general and we could be representing  $n$  components in the equations. For purely dispersive interactions, Eqs. 4 and 6 can be combined yielding:

$$W_a = 2\phi_1(\gamma_{S1}^D \gamma_L^D)^{1/2} + 2\phi_2(\gamma_{S2}^D \gamma_L^D)^{1/2} \quad (7)$$

We can express the total work of adhesion,  $W_a$ , to an effective surface energy of the mixture  $\gamma_{\text{eff}}^D$  (the net effect of the heterogeneous surface on the probe)

$$W_a = 2(\gamma_{\text{Seff}}^D \gamma_L^D)^{1/2} \quad (8)$$

Removing the common term, it is seen that the linear combination of the square roots of the surface area normalized dispersive energy terms are related to  $\gamma_{\text{eff}}^D$  as shown in Eq. 9. The general form of the equation for a mixture of  $n$  components each with a surface area fraction of  $\phi_n$  is presented in Eq. 10.

$$(\gamma_{\text{Seff}}^D)^{1/2} = \phi_1(\gamma_{S1}^D)^{1/2} + \phi_2(\gamma_{S2}^D)^{1/2} \quad (9)$$

$$(\gamma_{\text{Seff}}^D)^{1/2} = \sum_1^n \phi_n(\gamma_n^D)^{1/2} \quad (10)$$

Therefore, if surface energy values of the individual components ( $\gamma_n^D$ ) are known, it is possible to establish a calibration curve to determine surface fractions based on  $\gamma_S^D$  obtained for “unknown” samples.  $\gamma_{\text{Seff}}^D$  values measured for a series of physical mixtures with known  $\gamma_S^D$ , and  $\phi$  for the individual components will be used to validate Eq. 9.

## RESULTS AND DISCUSSION

**Producing a Calibration Curve for Surface Quantification: Lactose**

A useful application of Eq. 9 is for the quantification of amorphous content in a solid. Of course, given the nature of the measurement, we can only assess the surface amorphous content, and a separate bulk technique is required to fully characterize a powder. However, the ability to quantify the level of surface disorder is of interest in areas such as understanding the impacts of milling processes such as micronization, as well as aging processes post micronization. The approach to quantification will require crystalline and amorphous references for which we need to take the respective surfaces to be 100% crystalline or amorphous. It is important to note that the interpretation of results for unknown samples (*i.e.* a micronized sample) is in the context of the measured  $\gamma_S^D$  values for the reference crystalline and amorphous materials. As such, even if the material being measured contains a surface disorder other than a true amorphous phase (*i.e.* fractures, defect sites, or different exposed crystal planes) its energetics will be interpreted against the crystalline and amorphous references.

The initial test for the proposed model was carried out using lactose. Crystalline  $\alpha$ -lactose monohydrate and spray-dried lactose were taken as the crystalline, and a fully amorphous surface references, respectively. Confirmatory characterization was performed using solution calorimetry. The crystalline reference produced a  $\Delta H_{\text{soln}}$  value of 20.1 kJ/mol and the amorphous reference produced a  $\Delta H_{\text{soln}}$  value of -19.8 kJ/mol. These values are consistent with reported literature values for 100% crystalline and amorphous lactose (12). The materials were stored under vacuum as described in the materials section until processing—in particular to prevent surface recrystallization in the spray-dried material. The recorded SSA values for the crystalline and amorphous references were 0.3 and 1.8 m<sup>2</sup>/g, respectively.

Several physical mixtures were prepared using the reference materials, and Table I contains composition data of these samples, as well the  $\gamma_S^D$  for each and the crystalline and amorphous references. The  $\gamma_S^D$  values presented are the average of three repeat analyses, and the values following the means are the standard deviations. Also included in the table are  $\gamma_S^D$  values indicating the upper and lower values (range) obtained. The  $\gamma_S^D$  values range from 33.5 mJ/m<sup>2</sup> for the fully crystalline to 41.5 mJ/m<sup>2</sup> for the fully amorphous sample and the  $\gamma_S^D$  values for the physical mixtures fall within this range. Figure 1 shows the raw data presented in Table I compared against the theoretical plot of Eq. 9 where the SSA and  $\gamma_S^D$  values for the crystalline and amorphous references have

**Table I.**  $\gamma_s^D$  Values for Lactose Reference and Physical Mixture Samples ( $n=3$ )

Wt.% amorphous reference in binary mixture	Normalized amorphous surface area	Mean $\gamma_s^D$ /standard deviation (mJ/m <sup>2</sup> )	$\gamma_s^D$ range (mJ/m <sup>2</sup> )
0	0	33.52/0.69	33.29, 34.30
5.2	0.25	35.04/0.95	33.96, 35.43
10.2	0.41	36.10/0.63	35.37, 36.61
14.5	0.50	37.59/1.35	36.50, 39.10
50.0	0.86	40.06/0.01	40.02, 40.12
1	1	41.47/0.69	40.77, 41.89

been employed to generate the plot. The plot is generated for fractional amorphous SSA levels from 0.01 to 1 at increments of 0.01. As is readily seen, there is excellent agreement between experimental data and the theoretical prediction based on the surface energetics of the crystalline and amorphous references. Although the plot appears linear, the square root relationship produces a subtle curvature which would be more pronounced if the difference in the  $\gamma_s^D$  values for the reference materials were greater (9). The approach to using this calibration curve for amorphous quantification will be discussed in a following section.

### Producing a Calibration Curve: Drug Substance A

A second test of the utility of Eq. 9 for establishing a calibration curve was undertaken using an active drug substance. Amorphous and crystalline references were generated as discussed above. The amorphous and crystalline samples were characterized using XRPD. Figure 2 shows the diffractograms for each reference material. The crystalline reference displays well-resolved reflections consistent with crystalline material. The trace corresponding to the amorphous reference shows a halo rising above baseline consistent with material for which the long-range order in the lattice has been eliminated, i.e., X-ray amorphous. The recorded SSA values for the crystalline and amorphous references were 0.5 and 3.8 m<sup>2</sup>/g, respectively.

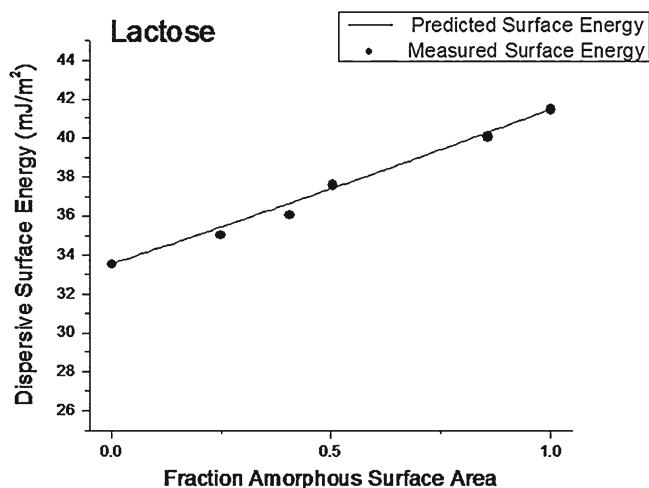


**Fig. 1.** Plot showing measured  $\gamma_s^D$  values for lactose physical mixture samples (points) compared to the predicted values based on Eq. 9 (line) as a function of fraction amorphous surface area

As with lactose, several physical mixtures were prepared using the reference materials and columns prepared as discussed previously. Table II contains composition data on the physical mixtures, as well the measured  $\gamma_s^D$  values for each sample and the crystalline and amorphous drug substance A references as obtained via IGC. The  $\gamma_s^D$  values range from 36.6 mJ/m<sup>2</sup> for the fully crystalline reference to 47.5 mJ/m<sup>2</sup> for the fully amorphous sample, and the  $\gamma_s^D$  values for the physical mixtures fall within this range. The values are the average of four repeat analyses, and as with Table I data relating to the standard deviation and range for each data set are also presented. Figure 3 shows the raw data presented in Table II compared against the theoretical plot of Eq. 9 where the SSA, and  $\gamma_s^D$  values for the crystalline and amorphous references have again been employed to generate the plot. As with the data for lactose shown in Figure 1, the plots are generated for fractional amorphous SSA levels from 0.01 to 1 at increments of 0.01. Again, there is good agreement between experimental data and the theoretical prediction based on the surface energetics of the crystalline and amorphous references. In this component of the work, it has been demonstrated that Eq. 9 has been employed on a second material to generate calibration plots suitable for quantification of surface amorphous content.

### EFFECTIVE AMORPHOUS SURFACE AREA

In the above theoretical section, it was shown that a reasonable quantitative model based on sound surface energetics theory could be developed. It was noted that by

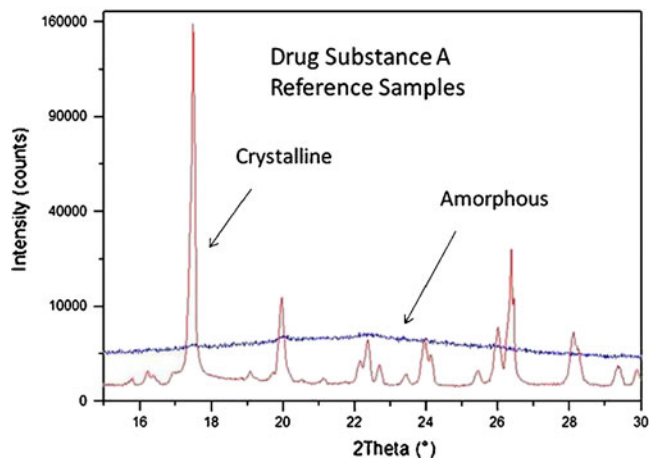


**Fig. 2.** Plot comparing the XRPD traces for the crystalline and amorphous reference samples of drug substance A

**Table II.**  $\gamma_S^D$  Values for Drug Substance A Reference and Physical Mixture Samples

Wt% amorphous reference in binary mixture	Normalized amorphous surface area fraction	Mean $\gamma_S^D$ /standard deviation (mJ/m <sup>2</sup> )	$\gamma_S^D$ range (mJ/m <sup>2</sup> )
0	0	36.60/1.50	34.94, 37.88
3.7	0.22	39.35/1.40	37.92, 40.71
8.5	0.41	40.33/1.31	38.25, 42.31
21.0	0.66	41.49/0.51	40.54, 42.58
48.7	0.88	45.64/0.46	45.22, 46.25
100	1	47.44/0.46	46.88, 47.76

using IGC—particularly in a Henry's region experiment—only information about the surface is obtained and this distinction must be made clearly. There are cases where it may be sufficient to only have knowledge of the surface. Alternatively, a complete picture may be necessary. In the first case, only IGC may be needed, however in the alternate case at least one additional bulk based technique (*e.g.* DSC) will be needed to produce a more complete picture of disorder throughout the particle.

In the theory section, the concept of effective surface energy was used to generalize the collective  $\gamma_S^D$  response. To further describe a surface in quantitative terms, we introduce EASA. In the above sections, the quantitative model utilized  $\gamma_S^D$  values for crystalline and amorphous references to produce curves which predicted the measured  $\gamma_S^D$  values of physical mixtures with good accuracy. The plots are suitable for use as calibration curves which can be employed to quantify the  $\gamma_S^D$  response obtained for an unknown.

Table III shows  $\gamma_S^D$  values for a series of lactose samples which have been processed in different ways: micronized, spray dried, and ball milled. The samples contain varying degrees of surface disorder, and the surface disorder has been quantified using the lactose calibration curve presented above. Of particular note is that the micronized sample was many months old, and the spray-dried sample had been allowed to partially re-crystallize. The aged micronized sample was found to have a  $\gamma_S^D$  of 35.6 mJ/m<sup>2</sup> which

produces an EASA of 28%. In other words, the samples displays a  $\gamma_S^D$  which is equivalent to a sample which would be made up of a surface area which is 28% amorphous and 72% crystalline *relative to the references used to produce the curve*. The sample could in fact have a different type of disorder present on the surface than that used as the reference; however, it has an effective surface energy energetically equivalent to a surface comprised of 28% of the amorphous phase used as the reference. Since we are locked with regard to the amorphous reference  $\gamma_S^D$  value, we can have responses >100% of EASA. These present no particular issue, the ball-milled sample shown in Table III (EASA=120%) can be rationalized as a surface which is 1.2 times as energetic as the amorphous reference employed with regards to  $\gamma_S^D$ . The partially recrystallized spray-dried sample produces an intermediate  $\gamma_S^D$  value of 39.5 mJ/m<sup>2</sup>. This value equates to an EASA value of 77%—or a surface which has the effective surface energy of one which is 77% amorphous and 22% crystalline relative to reference materials used.

In Table III, quantitative values of bulk amorphous content are displayed derived from solution calorimetry data. These values are obtained in the same manner as with those for the crystalline and amorphous references as described above (12). The combined set of IGC and solution calorimetry data produces a more thorough assessment of how disorder is dispersed in the particles investigated. For the aged micronized sample with a  $\Delta H_{\text{soln}}$  of 20.1 kJ/mol, we can describe a system with a moderately disordered surface (EASA ~30%) but with no measurable disorder in the bulk. Therefore, the disorder is likely to reside only at the surface of these particles. The partially recrystallized spray-dried particles can be described as having an energetic surface (EASA approaching 80%) as well as bulk containing a significant amorphous percentage (~70%). Interestingly, the surface and bulk values are comparable. The ball milled sample has a very highly energetic surface (EASA of 120%) while showing a small but measurable amount of bulk disorder (~5%). In this case, the sample may be comprised of a highly disordered surface with perhaps a few tenths of microns of depth of this disorder. For example, assuming a

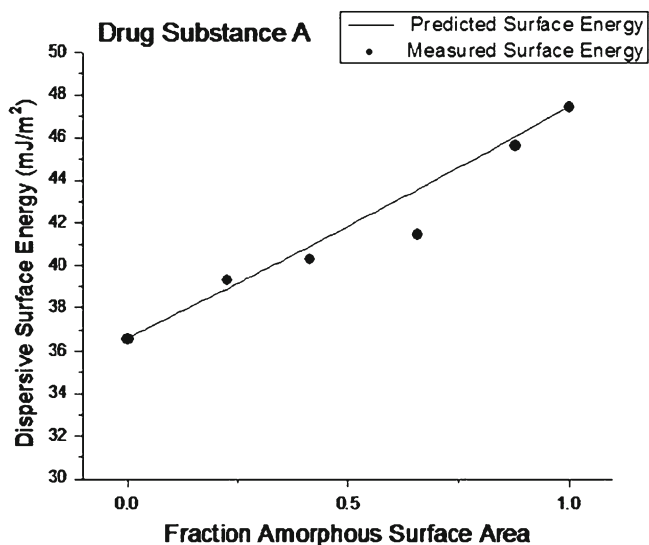


**Fig. 3.** Plot showing measured  $\gamma_S^D$  values for drug substance A physical mixture samples (points) compared to the predicted values based on Eq. 9 (line) as a function of fraction amorphous surface area

**Table III.** EASA Values and Approximate Bulk Amorphous Content for Various Processed Lactose Samples

Sample	$\gamma_D$ (mJ/m <sup>2</sup> )	EASA	$\Delta H_s$ (KJ/mol)	Bulk% amorphous
Micronized	35.6	28%	20.1	~0
Spray dried	39.5	77%	-8.4	72
Ball milled	43.1	120%	18.3	5

spherical particle with a diameter of 5  $\mu\text{m}$ , the thickness of a disordered shell providing a bulk amorphous response of  $\sim 5\%$  would be between 0.2 and 0.3  $\mu\text{m}$  based on the  $\Delta H_{\text{soln}}$  values of the crystalline and amorphous references. An alternative path to this type of result would be exposure or increased exposure of facets with relatively stronger van der Waals interactions which could have occurred during the milling process (13).

These results present a preliminary example of how bulk and surface measurements can be combined to produce a thorough view of how disorder is dispersed through a sample particle. An assessment of particle shape and size will produce an even more detailed picture. This will be the topic of future investigations.

## CONCLUSION

An approach to quantifying surface amorphous content has been presented and demonstrated for two systems. The approach is based on the idea of effective surface energy produced by Sun and Berg for understanding dispersive surface energy results from measurements on heterogeneous mixtures of materials (9). It was further discussed that with quantifying "amorphous" content by this approach, it must be understood that we are limited to describing the nature of surface of an unknown to the context of our reference materials. An actual processed particle surface may not contain true phase separated amorphous material, but we can describe its energetics in terms of the reference materials based on effective amorphous surface area. In addition, we showed that by combining surface data with bulk amorphous quantification data a more thorough picture of how disorder is distributed throughout a particle is achieved.

## ACKNOWLEDGMENTS

The authors would like to thank Dr. Rachel Forcino, and Ms. Maria Barnett for supplying the samples of Drug Substance A, and amorphous lactose respectively. We also thank the reviewers for constructive comments.

## REFERENCES

1. Buckton G, Dove J, Davies P. Isothermal microcalorimetry and inverse phase gas chromatography to study small changes in powder surface properties. *Int J Pharm.* 1999;193:13–9.
2. Buckton G, Ambarkhane A, Pincott K. The use of inverse gas chromatography to study the glass transition temperature of a powder surface. *Pharm Res.* 2004;9:1554–7.
3. Adamska K, Voelkel A. Inverse gas chromatographic determination of solubility parameters of excipients. *Int J Pharm.* 2005;304:11–7.
4. Adamska K, Voelkel A, Heberger H. Selection of solubility parameters for characterization of pharmaceutical excipients. *J Chromatogr A.* 2007;1171:90–7.
5. Newell H, Buckton G, Butler D, Thielmann F, Williams D. The use of inverse phase gas chromatography to study the change in surface energy of amorphous lactose as a function of relative humidity and the process of collapse and crystallization. *Int J Pharm.* 2001;217:45–56.
6. Planinsek O, Buckton G. Invergas chromatography: considerations about appropriate use for amorphous and crystalline powders. *J Pharm Sci.* 2003;92:1286–94.
7. Newell H, Buckton G. Inverse gas chromatography: investigating whether the techniques preferentially probes high energy sites for mixtures crystalline and amorphous lactose. *Pharm Res.* 2004;8:1440–4.
8. Adamson A, Gast AP. *Physical chemistry of surfaces.* 6th ed. New York: Wiley; 1997.
9. Sun C, Berg J. The effective surface energy of heterogeneous solids measured by inverse gas chromatography at infinite dilution. *J Colloid Interface Sci.* 2003;260:443–8.
10. van Oss C, Good R. Surface tension and solubility of polymers and biopolymers: the role of polar and apolar interfacial free energies. *Journal of Macromolecular. Science. Chemistry.* 1989;26:1183–203.
11. Schultz J, Lavielle L. Inverse gas chromatography: characterization of polymers and other materials. In: Lloyd D, Ward T, Schreiber H, editors. *ACS Symposium Series 391.* Washington DC: American Chemical Society; 1989.
12. Hogan S, Buckton G. The quantification of small degrees of disorder in lactose using solution calorimetry. *Int J Pharm.* 2000;207:57–64.
13. Ho R, Wilson D, Heng J. Crystal habits and the variation in surface energy heterogeneity. *Cryst Growth and Des.* 2009;9:4907–11.